ESA_QCA00174_M00

HIGH-ENERGY BORON-IMPLANTATION AND PROTON-IRRADIATION EFFECTS IN DIODES WITH SHALLOW TRENCH ISOLATION

A. Poyai[1], E. Simoen and C. Claeys[1]
IMEC, Kapeldreef 75, B-3001 Leuven, Belgium
[1]also at EE Dept., KU Leuven, Kard. Mercierlaan 94, B-3001 Leuven, Belgium

K. Hayama, K. Kobayashi and H. Ohyama
KNCT, 2659-2 Nishigoshi, Kumamoto 861-1102 Japan

H. Takizawa
Takasaki JAERI, 1233 Watanuki Takasaki Gunma, 370-1292 Japan

M. Kokkoris, E. Kossionides and G. Fanourakis
NCSR 'Demokritos', Ag. Paraskevi Attikis, 153 10 Athens, Greece

A. Mohammadzadeh
ESTEC-ESA, Keplerlaan 1, Noordwijk, The Netherlands

ABSTRACT

This paper describes the current-voltage characteristics of n^+-p junctions surrounded by shallow trench isolation (STI), both before and after high-energy proton irradiation. Particular emphasis is on the lifetime properties of the bulk p-well region, which has been fabricated by a deep (200 keV) and a shallow (55 keV) boron ion implantation. It will be demonstrated that before irradiation, the leakage current of large area diodes is governed by residual, unannealed deep B-implantation damage. This is derived from Deep Level Transient Spectroscopy (DLTS) analysis and further supported by the temperature dependence of the volume leakage current. After 8, 20 or 60 MeV proton irradiation, the leakage-current Arrhenius plot shows a different activation energy, demonstrating the impact of radiation-induced deep levels. At the same time, ionisation damage has been created in the STI oxide regions, enhancing the surface generation and, hence, the peripheral leakage current component.

INTRODUCTION

Scaling of CMOS remains the main microelectronics technology drive for the next decade. In order to be able to further shrink the device feature size and increase the integration density some barriers have to be overcome, which require new, alternative processing steps. One key issue is the device isolation, which was formerly achieved by a LOCal Oxidation of Silicon (LOCOS) scheme. For sub-0.25 μm technologies, it has become clear that it is more and more difficult to control the lateral oxidation, giving rise to the bird's beak of the field oxide and, hence, limiting

the minimum active-device spacing. A good alternative, therefore, is the use of shallow trench isolation (STI), which consists basically of dry-etching a shallow (0.2-0.4 μm) trench in the silicon, followed by a thermal oxidation of the sidewalls at high temperatures and finally, filling the trench by a deposited oxide (TEOS). This yields an essentially bird's beak-free structure (Fig. 1) which allows better scaling and planarisation. The latter is particularly important for subsequent Chemical Mechanical Polishing (CMP) treatments. One feature in STI requiring special attention is the mechanical stress associated with the isolation structure, which may induce extended-defect formation in the adjacent silicon substrate or cause enhanced interface-state formation at the oxide-silicon interface. This in turn may determine the leakage current in a p-n junction isolated by STI regions. Particularly the surface generation-recombination (GR) current, scaling with the diode perimeter P will be governed by the electrical properties of the device isolation.

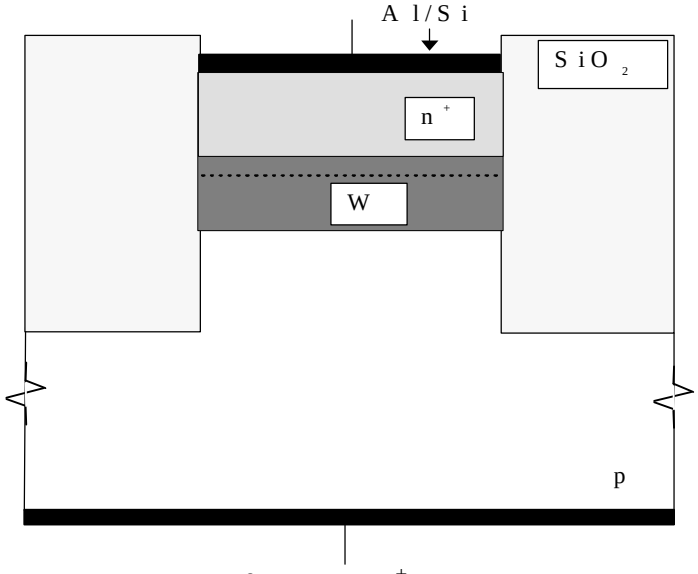

Fig. 1: Schematical representation of an STI n^+-p diode. W is the width of the depletion region.

Scaling the gate oxide thickness of deep submicron CMOS is also advantageous for future space applications. When the thickness t_{ox} becomes below the tunneling limit of 6 nm, no long-term charge trapping occurs during high-energy particle or photon irradiation, so that this degradation mechanism can be in first instance neglected. However, as the device isolation is still using rather thick (lower-quality) oxides, ionisation damage in these edge regions is still a problem (for an overview see e.g. Ref. 1). As a result, irradiated submicron transistors will suffer from subthreshold (edge) leakage, which will be particularly detrimental for the off-state power consumption [2-3]. For certain applications, this can be overcome by using edgeless devices, which is traded for the density of the design. However, for high-density applications or Custom-of-the Shelf (COTS) parts, hardening of the isolation is more an issue than ever, especially in the light of replacing LOCOS by STI [1-4]. Initial studies have revealed that STI is prone to ionisation damage [4], which relies strongly on the processing details (edge rounding, over- or underfilled trenches…). So far, only the impact of high-energy gamma or X-ray irradiation on the performance of STI MOSFETs has been studied [2-4]. For space applications, also high-energy

protons should be considered. Therefore, it is the aim of the paper to investigate the impact of STI on the electrical performance of deep-submicron CMOS-compatible shallow n^+-p junction diodes schematically shown in Fig. 1, both before and after high-energy proton irradiation. This is a first step in the space-radiation evaluation of the next-generation 0.13-0.15 μm CMOS technology under development at IMEC.

EXPERIMENTAL

The junctions have been processed in a retrograde p-well, obtained by a deep (200 keV, $1.2x10^{13}$ cm^{-2}) and a shallow (55 keV, $1.5x10^{13}$ cm^{-2}) B ion implantation, followed by a dopant activation anneal (10 min, 850°C). For the n^+-layer, an As ion implantation (70 keV, $4x10^{15}$ cm^{-2}) and anneal (10 s, 1100°C) was performed, resulting in a junction depth of around 0.11 μm. This was followed by a 15 nm Co silicidation, using an 8 nm Ti cap. The active regions were defined by STI, processed according to different splits. Diodes with different Area (A) to Perimeter (P) ratio were fabricated, enabling to separate the area bulk leakage current density J_A (A/cm^2) from the peripheral leakage current density J_P (A/cm), based on the procedure described elsewhere [5-6]. Particularly the latter component should be sensitive to ionisation damage in the STI regions. In addition to standard current-voltage (I-V) and capacitance-voltage (C-V) measurements, also temperature-dependent measurements were performed in the range 25 to 120°C, allowing to extract the activation energy of the reverse current density. Finally, a more detailed analysis of the microscopic nature of the pre- and post-rad damage was pursued by a combination of Deep Level Transient Spectroscopy (DLTS) and Transmission Electron Microscopy (TEM).

The 20 MeV proton irradiations took place at the Takasaki JAERI, while 8 MeV exposures were undertaken at Demokritos. The fluence range was 10^{12}, 10^{13} and 10^{14} cm^{-2} in the first case and $5x10^{11}$, $5x10^{12}$, $5x10^{13}$ cm^{-2} in the latter. Finally, 60 MeV proton exposures were performed up to a fluence of $5x10^{11}$ cm^{-2}, using the Cyclone facility in Louvain-la-Neuve. No bias was applied during the irradiations. The experimental diode degradation at different proton energies has been compared with the calculated Non-Ionising Energy Loss (NIEL) parameter [7-8], in order to find out whether it scales with the induced displacement damage.

RESULTS AND DISCUSSION

Pre-rad Characterisation

Typical I-V characteristics before irradiation are shown in Fig. 2 for a 10 mm^2 SQ1 diode, from which no marked impact of the STI processing is observed. For such large-area diodes, the reverse current is dominated by the area generation current density J_{gA}, explaining the absence of any peripheral isolation effect. Diodes with a good ideality (ideality factor m 1) were obtained. However, comparing with the leakage current of a similar diode, fabricated in a lowly-doped p-type substrate shows a substantial increase in J_{gA} or a corresponding reduction in the generation lifetime τ_g for the STI case [6]. In the frame of the Shockley-Read-Hall (SRH) model the latter parameter can be approximated by:

$$\tau_g = \tau_r \exp(|E_T-E_i|/kT) = (N_T \sigma v_{th})^{-1} \exp(|E_T-E_i|/kT) \quad (1)$$

with τ_r the recombination lifetime which can be derived from the diffusion current component [5], N_T the generation centre concentration, σ the corresponding capture cross section, v_{th} the carrier thermal velocity (~10^7 cm/s), E_T the trap energy level and E_i the intrinsic Fermi level position. Finally, k is the Boltzmann constant and T the absolute temperature. The enhanced J_{gA} points to the presence of a high density of Generation-Recombination (GR) centres in the depletion region of a diode with a p-well.

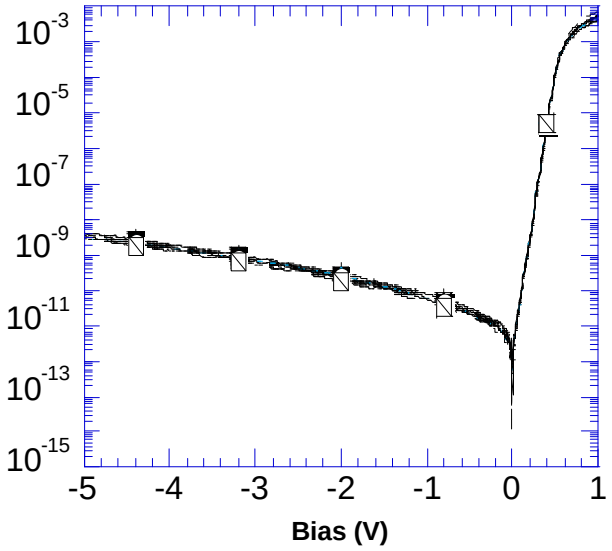

Fig. 2: I-V characteristics for different STI splits at 25°C and for a diode area of 10 mm^2 (SQ1 structure).

A first simple method to assess the responsible GR centres is the study of the temperature dependence of J_{gA} for not too high reverse bias V_R, in order to reduce possible electric-field enhanced carrier generation in the depletion region (p-well). This leads to the result of Fig. 3 at a V_R=-1 V. There, the normalised generation current density is represented, to take account of the prefactor T-dependence [5], both for the volume generation (J_{gA}) and diffusion (J_{dA}) current density. The latter has been derived from the forward current intercept in the ideal exponential region, corresponding to an ideality factor m=1. As can be seen, J_{dA} dominates at higher temperatures and gives rise to an activation energy close to the band gap of silicon (1.12 eV). At lower T, the generation current governs the leakage of an area diode and yields an effective activation energy of 0.28 eV. In other words, the generation centers are apparently at 0.28 eV from either the valence or the conduction band.

Standard capacitance DLTS measurements of several 2 mm^2 STI p-well diodes reveal the presence of a broad distribution (in energy) of hole traps, ranging from about 300 meV up to 500 meV above the valence band E_v (Fig. 4). In addition, studying the concentration profile in function of the quiescent reverse bias demonstrates the non-uniform trap distribution in the depletion region. This follows for example from the fact that the spectrum is more or less flat close to the junction (-1→0V curve), while a clear peak is seen at a larger average depletion depth from –4→+0.1 V. The estimated N_T is on the order of 0.1 % of the p-well doping density,

i.e. around $2x10^{14}$ cm^{-3}. On the other hand, no deep levels have been observed in the non p-well control diodes above 100 K. The fact that the trap density is non-uniform and occurs for a depth close to the projected range of the 200 keV B-implantation suggests that these hole traps may correspond to residual damage, possibly small interstitial aggregates. In the literature, similar result like in Fig. 4 have been obtained [9-11], although much higher activation energies were found, around 0.65 and 0.67 eV for 0.7 MeV and 950°C (20 min) annealed deep B implantations [10]. In another report, corresponding with a 150 keV B- implantation, followed by a 10 s 1100°C rapid thermal anneal, a hole trap at E_v+0.350 eV was observed [12], in the range of our observations.

From recent studies of interstitial-related defects in high-energy ion–implanted p-type silicon, it has become clear that a whole family of trap levels can be formed, depending on the applied thermal budget [13-15]. The higher the annealing temperature, the larger the size of the remaining interstitial aggregates/clusters [13]. In the end, the size of the extended defects may be large enough to be observable with TEM. However, TEM analysis on an STI diode did not reveal any extended defects at the depth of interest below the surface. This is in agreement with previous reports [9-11], demonstrating the electrical activity of small B-implantation related clusters, which size is too small to be detected by TEM. It should also be emphasised that as yet, no logarithmic capture processes, typical for dislocation (loops) and extended defects have been found. The trap filling kinetics seems to follow the standard exponential law for point defects.

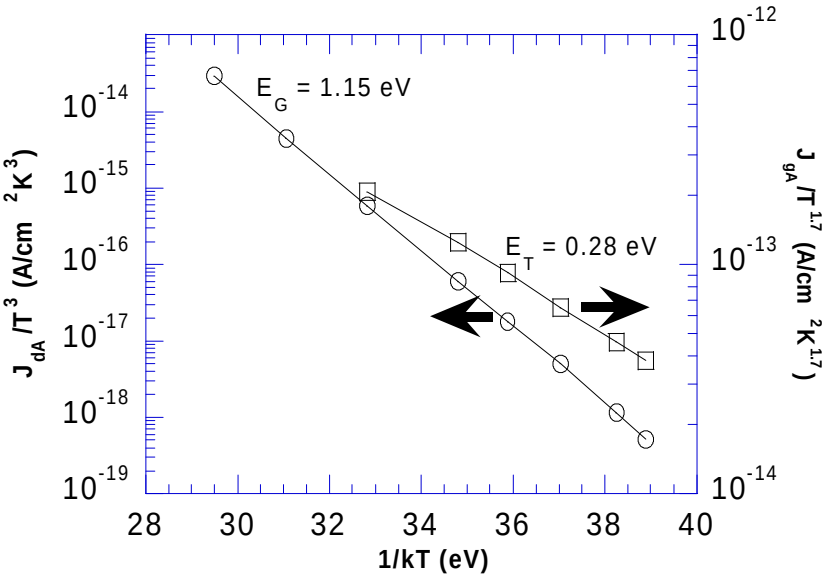

Fig. 3: Arrhenius plot of the temperature-normalised volume diffusion (J_{dA}) and generation current density (J_{gA}) of a 10 mm^2 n^+-p STI junction. V_R=-1 V.

A few comments should be made with respect to the correlation between the temperature-dependent I-V measurements and the DLTS results. The activation energy shown in Fig. 3 is at the lower end of the range of hole trap energies of Fig. 4, which is rather surprising. One normally expects that the more close to mid gap (i.e. an activation energy of 0.56 eV), the more efficient generation centre is obtained.

From this, one could conclude that the actual leakage-current-generation centres at an effective energy of E_v+ (or E_c-)0.28 eV are different than the deep levels found in DLTS. More work is needed to clarify this point. However, it has become clear that for sufficiently large reverse bias, transient phenomena are observed in the reverse current characteristics of the STI diodes [16], which are associated with hole trapping by the ion-implantation related defects. In addition, to correctly model the leakage current, one should consider the distribution of the B-implantation related traps both in energy and in depth.

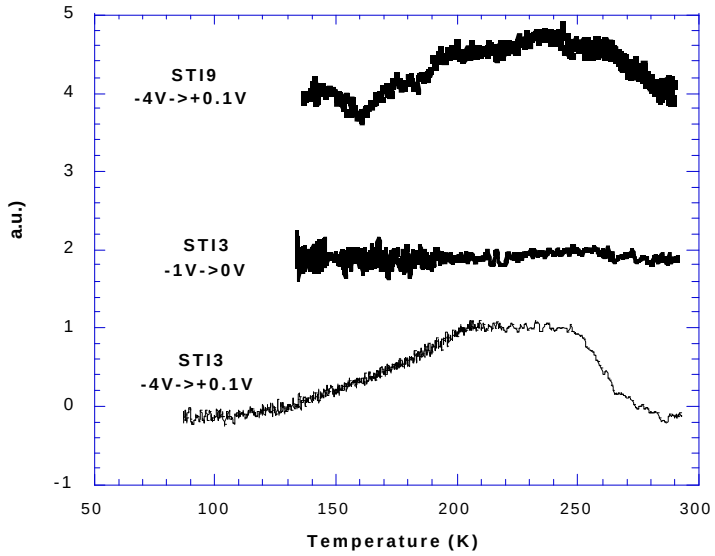

Fig. 4: DLTS spectra of different unirradiated STI diodes (A=2 mm^2) showing the presence of a broad distribution of hole traps at some distance of the junction. The voltage pulse duration was 1 ms and the time constant window 6 ms.

Post-rad Characterisation

After proton irradiation, a clear increase of both the forward and reverse current is observed in Fig. 5 a and 5b, corresponding with 20 and 8 MeV proton irradiations, respectively. However, for sufficiently large forward bias, the forward current in Fig. 5a reduces after irradiation, indicating an increase of the series resistance. This could for example result from a deactivation of the boron concentration ([B]) in the p-well. High-frequency (100 kHz) C-V measurements support this idea: the capacitance of the reversely biased diodes reduces with proton fluence. A lowering by a factor 2 has been reported after a 10^{13} cm^{-2} 20 MeV proton irradiation, corresponding to a reduction by a factor 4 of the active dopant concentration in the p-well [17]. This deactivation is thought to proceed according to the interaction with radiation-induced interstitials (I):

$$B_s + I \rightarrow Si + B_i \qquad (2)$$

whereby a substitutional B atom (B_s) is kicked out of its lattice site by a silicon interstitial, generating a mobile and inactive B interstitial (B_i). B_i can subsequently

react with other impurities, generating more stable radiation complexes like B_iB_s, B_iO_i, B_iC_s,….

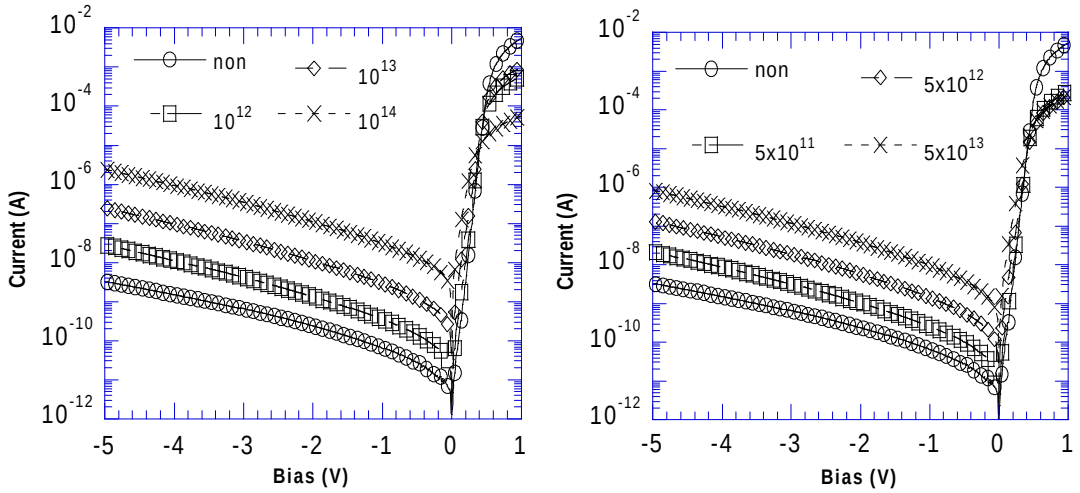

Fig. 5: I-V characteristics of 10 mm^2 n$^+$-p diode after a 20 MeV proton irradiation, for different fluences and 25°C (a) and after an 8 MeV proton irradiation (b).

The increase in reverse current for a large area diode scales roughly with the fluence Φ, as shown more explicitly in Fig. 6 for a V_R=-1 V. The slope of the straight-line fit to the data points gives the reverse-current damage coefficient K_I, defined by:

$$K_I = I_R / \Phi \quad \Delta I_R/\Delta\Phi \qquad (3)$$

which is proportional to the generation-lifetime damage coefficient $K_{\tau g}$ in first instance. The increase of the leakage current and of the forward current in Fig. 5 is mainly due to a decrease of the generation and recombination lifetime, respectively. However, the deactivation of the boron will in turn cause an increase of the depletion width for the same reverse bias. This should eventually cause a non-linear change in I_R at the largest fluences.

The damage coefficients corresponding with the data of Fig. 5 are summarised in Table I and compared with the NIEL parameter [8]. Surprisingly, no proportionality is observed between K_I and NIEL, which is expected if the main degradation mechanism is due to lattice damage in the bulk. One possible explanation may be the occurrence of ionisation damage in the STI oxides, which causes an increase of the peripheral leakage current. Evidence for that is provided in Fig. 5a or 5b for example, showing the development of a clear non-ideal recombination component in forward operation at low bias, which is generally associated with interface states. Therefore, we should compare the NIEL with the damage coefficient for the volume leakage current, which can be separated by combining the data of different-geometry diodes [5-6]. Unfortunately, for the 8 MeV diodes only part of the structures were irradiated because of the small beam diameter, so that the analysis can not be performed. However, for these large-area SQ1 diodes, it is anticipated that in principle the perimeter component is negligible even after proton irradiation. Another

factor which may play is the B-deactivation mentioned above. Currently, further C-V analysis is undertaken to study the K_B damage coefficient (=-[B]/ Φ) and its relationship with NIEL.

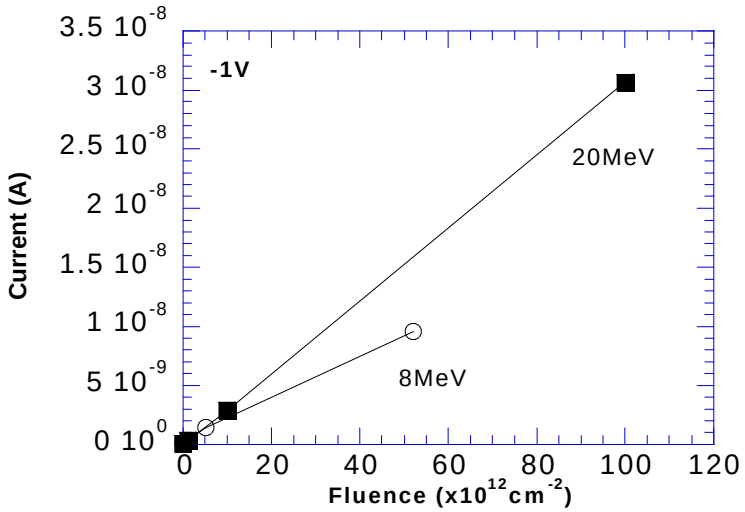

Fig. 6: Leakage current at V_R=-1 V and 25°C of 8 MeV and 20 MeV proton-irradiated SQ1 STI diodes in function of the fluence.

Table I : Leakage-current damage coefficient obtained at –1 V for proton-irradiated 10 mm^2 large-area diodes, compared with the theoretical total NIEL (after [8]).

Proton Energy (MeV)	K_I (A cm^2/proton)	NIEL (keV cm^2/g)
8	1.8×10^{-22}	9.49
20	3.1×10^{-22}	5.36
60	2.8×10^{-22}	3.52

In order to derive the activation energy of the generation current density, temperature-dependent measurements have been performed for the 20 MeV STI diodes. A result obtained for a reverse bias of -1 V and a fluence $\Phi=10^{13}$ cm^{-2} is given in Fig. 7. It is clear that after irradiation, the generation current dominates in the whole temperature interval, giving rise to activation energies in the range 0.49 to 0.66 eV, i.e. near mid gap, which explains the drastic increase of J_{gA}. The different energy level E_T after proton exposure indicates that radiation-induced centres are mainly responsible for the leakage current increase in Fig. 5, overwhelming the effect of the pre-existing deep levels shown in Fig. 4. Although no DLTS results are available yet, one can anticipate that the divacancy level at E_c-0.42 eV will play an important role

[18-21], eventually assisted by some other deep traps, possibly associated with B_I or its stable complexes. It should finally be noted that after the temperature-dependent I-V measurements, a reduction of the leakage current of no more than 10% has been found [17], indicating some annealing of radiation defects.

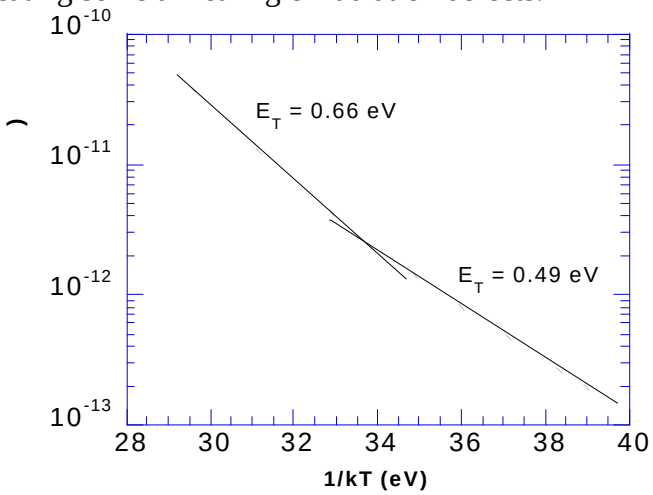

Fig. 7: Arrhenius plot of the generation current density after a 20 MeV 10^{13} cm^{-2} proton irradiation. V_R=-1 V.

The occurrence of ionisation damage can be investigated by studying the peripheral leakage current component (I_P) of large-perimeter diodes. This should give an idea of the charge-trapping and interface-state generation properties of proton-irradiated STI oxides. An example is given in Fig. 8, after 20 MeV proton exposure. Again, a linear increase of I_P with Φ is observed, which enables to derive a corresponding damage coefficient. The slopes indicated in Fig. 8 are for a proton fluence of 10^{12} cm^{-2} and show a strong dependence on the reverse bias. This suggests a field-dependent non-SRH generation mechanism to be responsible for the surface generation current. It has also been found that the STI processing has a marked impact on the ionisation damage [17], in agreement with recent reports [3-4].

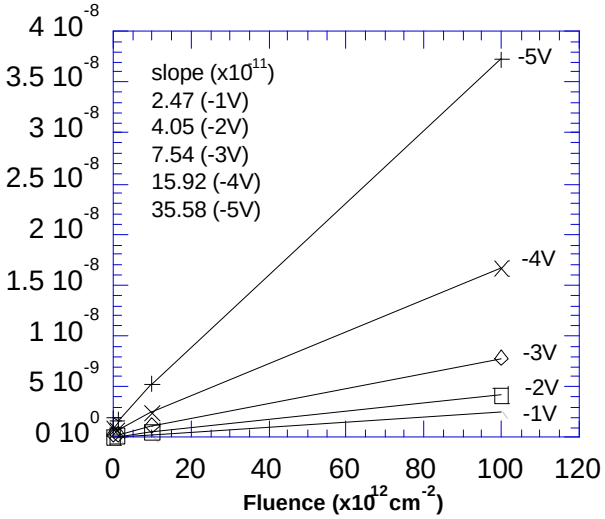

Fig. 8: Increase in the reverse current of a meander diode at different reverse bias, in function of the 20 MeV proton fluence. T=25°C.

CONCLUSION

Summarising, a clear degradation of the forward and reverse characteristics of high-energy proton irradiated diodes with STI has been observed. Both the area and the peripheral leakage current component increase significantly, implying the occurrence of displacement and ionisation damage, respectively.

ACKNOWLEDGEMENTS

The Authors are indebted to the CMOS group and in particular G. Badenes and R. Rooyackers for supplying the wafers and the relevant technological information. In addition, we wish to thank P. van Dorpe and G. Berger for assistance during the electrical measurements and the 60 MeV proton irradiations, respectively. H. Bender kindly performed the TEM analysis. This work, carried out within the ENDEASD Network, has partly been financed by ESTEC under Work Order 1938/96/NL/LB. A. Poyai is indebted to the Thai government for his scholarship supported through the National Science and Technology Agency (NSTDA) of Thailand. K. Chumsri kindly performed the electrical measurements of the 60 MeV proton irradiated diodes.

REFERENCES

1. C. Claeys and E. Simoen. *Literature Study on Radiation Effects in Advanced Semiconductor Devices*, Chapter 4, Doc no P35284-IM-RP-0016 (March, 2000).
2. J. Maimon and N. Haddad. *IEEE Trans. Nucl. Sci.* **46**, 1686 (1999).
3. F.T. Brady, J.D. Maimon and M.J. Hurt. *IEEE Trans. Nucl. Sci.* **46**, 1836 (1999).
4. M.R. Shaneyfelt, P.E. Dodd, B.L. Draper and R.S. Flores. *IEEE Trans. Nucl. Sci.* **45**, 2584 (1998).
5. A. Poyai, E. Simoen, C. Claeys and A. Czerwinski. *Materials Science and Engin.* **B73**, 191 (2000).
6. A. Poyai, E. Simoen, R. Rooyackers, G. Badenes and C. Claeys. to be published in the *Proc. of Symposium M of the E-MRS Spring Meeting*, Strasbourg (France), 30 May-2 June, 2000.
7. G.P. Summers, E.A. Burke, C.J. Dale, E.A. Wolicki, P.W. Marshall and M.A. Gehlhausen. *IEEE Trans. Nucl. Sci.* **34**, 1134 (1987).
8. C.J. Dale, L. Chen, P.J. McNulty, P.W. Marshall and E.A. Burke. *IEEE Trans. Nucl. Sci.* **41**, 1974 (1994).
9. H. Sayama, M. Takai, Y. Akasaka, K. Tsukamoto and S. Namba. *Japan. J. Appl. Phys.* **28**, L1673 (1989).
10. H. Sayama, M. Takai, Y. Yuba, S. Namba, K. Tsukamoto and Y. Akasaka. *Appl. Phys. Lett.* **61**, 1682 (1992).
11. H. Sayama, A. Kinomura, Y. Yuba and M. Takai. *Nucl. Instrum. Methods in Phys. Res.* **B80/81**, 587 (1993).
12. S. Dueñas, E. Castán, L. Enríques, J. Barbolla, J. Montserrat and E. Lora-Tamayo. *Semicond. Sci. Technol.* **9**, 1637 (1994).
13. J.L. Benton, K. Halliburton, S. Libertino, D.J. Eaglesham and S. Coffa. *J. Appl. Phys.* **84**, 4749 (1998).

14. S. Libertino, J.L. Benton, D.C. Jacobson, D.J. Eaglesham, J.M. Poate, S. Coffa, P.G. Fuochi and M. Lavalle. *Appl. Phys. Lett.* **70**, 3002 (1997).
15. S. Fatima, J. Wong-Leung, J. Fitz Gerald and C. Jagadish. *Appl. Phys. Lett.* **72**, 3044 (1998).
16. A. Poyai, E. Simoen and C. Claeys. Paper submitted to *Appl. Phys. Lett.*
17. E. Simoen, A. Poyai and C. Claeys. *Radiation Damage Studies in Advanced Microelectronic Materials and Devices*, Doc. No P35284-IM-RP-0018 (29 February 2000).
18. P.F. Lugakov, T.A. Lukashevich and V.V. Shusha. *Phys. Stat. Sol. A.* **74**, 445 (1982).
19. E. Simoen, J. Vanhellemont and C. Claeys. *Appl. Phys. Lett.* **69**, 2858 (1996).
20. E. Simoen, C. Claeys and H. Ohyama. *IEEE Trans. Nucl. Sci*. **45**, 89 (1998).
21. E. Simoen, C. Claeys, E. Gaubas and H. Ohyama. *Nucl. Intrum. Meth. Phys. Res. A.* **439**, 310 (2000).

Keywords

Shallow Trench Isolation

Displacement Damage

NIEL

Boron Ion Implantation

P-well

Interstitial defects/clusters

B deactivation